

# Hyperfine structure and electric quadrupole transitions in the deuterium molecular ion

P. Danev and D. Bakalov\*

*Institute for Nuclear Research and Nuclear Energy, Bulgarian Academy of Sciences,  
blvd. Tsarigradsko ch. 72, Sofia 1142, Bulgaria*

V.I. Korobov

*Bogoliubov Laboratory of Theoretical Physics, Joint Institute for Nuclear Research, 141980, Dubna, Russia*

S. Schiller

*Institut für Experimentalphysik, Heinrich-Heine-Universität Düsseldorf, 40225 Düsseldorf, Germany*

(Dated: June 29, 2020)

Molecular hydrogen ions are of metrological relevance due to the possibility of precise theoretical evaluation of their spectrum and of external-field-induced shifts. In homonuclear molecular ions the electric dipole  $E1$  transitions are strongly suppressed, and of primary laser spectroscopy interest is the electric quadrupole ( $E2$ ) transition spectrum. In continuation of previous work on the  $H_2^+$  ion, we report here the results of the calculations of the rate of laser-induced electric quadrupole transitions between a large set of ro-vibrational states of  $D_2^+$ . We also present an evaluation of the hyperfine structure that corrects errors in previous publications in the literature. The effects of the laser polarization in the hyperfine and Zeeman structure of the  $E2$  transition spectrum are treated in detail.

## I. INTRODUCTION

Molecular hydrogen ions (MHIs) are three-body systems that offer the possibility for both high precision spectroscopy [1, 2] and accurate theoretical evaluation of the spectrum and shifts due to external fields. The comparison of currently available and future high precision experimental and theoretical results has the potential to provide more accurate values of fundamental constants, such as the Rydberg constant, proton-to-electron and deuteron-to-electron mass ratios, etc. Transitions with low sensitivity to external fields are promising candidates for the search for a time-variation of the mass ratios. For recent progress in the field and the perspectives opened, see e.g. Refs. [3, 4, 9].

Of main interest in the case of homonuclear MHIs ( $H_2^+$ ,  $D_2^+$ ) are the electric quadrupole ( $E2$ ) spectra. The first calculations in the approximation of spinless particles were performed back in 1953 by Bates and Poots [5], followed by works of Posen et al. [6], Pilon and Baye [7], and Pilon [8]. The hyperfine structure (HFS) of the  $E2$ -spectral lines of  $H_2^+$  was first considered in [9] and systematically investigated in [10].

In the present work, we extend the approach of [10] to the deuterium ion  $D_2^+$ . In Sec. II, we re-evaluate the HFS of  $D_2^+$  in the Breit-Pauli approximation since the results of the preceding works [11–13] need corrections. Sec. III is dedicated on the study of the laser-stimulated  $E2$  transition spectrum in  $D_2^+$  with account of the HFS of the molecular levels and the polarization of the laser source. In the final Sec. IV we summarize and discuss the results.

## II. HYPERFINE STRUCTURE OF DEUTERIUM MOLECULAR ION

### A. Theoretical model

The nonrelativistic Hamiltonian of the hydrogen molecular ion  $D_2^+$  is:

$$H^{\text{NR}} = \frac{\mathbf{p}_1^2}{2m_d} + \frac{\mathbf{p}_2^2}{2m_d} + \frac{\mathbf{p}_e^2}{2m_e} + \frac{e^2}{4\pi\epsilon_0} \left( -\frac{1}{r_1} - \frac{1}{r_2} + \frac{1}{r_{12}} \right), \quad (1)$$

where  $m_d$  and  $m_e$  are the masses of the deuterons and the electron,  $\mathbf{R}_1$ ,  $\mathbf{R}_2$ ,  $\mathbf{R}_e$  and  $\mathbf{p}_1$ ,  $\mathbf{p}_2$ ,  $\mathbf{p}_e$  are the position and momentum vectors of the two deuterons and the electron in the center of mass frame, and  $\mathbf{r}_{1,2} = \mathbf{R}_e - \mathbf{R}_{1,2}$ ,

---

\*Electronic address: bakal10@abv.bg

$\mathbf{r}_{12} = \mathbf{R}_2 - \mathbf{R}_1$ ,  $r_{1,2} = |\mathbf{r}_{1,2}|$ ,  $r_{12} = |\mathbf{r}_{12}|$ . We consider only  $\Sigma_g$  states of  $D_2^+$ ; in the nonrelativistic approximation the discrete  $\Sigma_g$  states of the hydrogen isotope molecular ions are labeled with the quantum numbers of the nuclear vibrational excitation  $v$ , of the total orbital momentum  $L$ , and of its projection on the space-fixed quantization axis  $L_z$ ; the spatial parity  $\lambda = \pm 1$  is constrained to  $\lambda = (-1)^L$  and will be omitted in further notations. The nonrelativistic (Coulomb) energy levels and wave functions of  $D_2^+$  in the state  $|vLL_z\rangle$  are denoted by  $E^{(\text{NR})vL}$  and  $\Psi^{(\text{NR})vLL_z}$ , respectively.

The leading-order spin effects are described by adding to  $H^{\text{NR}}$  the pairwise spin interaction terms  $V$  of the Breit-Pauli Hamiltonian of Ref. [14]:

$$H = H^{\text{NR}} + V, \quad V = V_{ed_1} + V_{ed_2} + V_{dd}, \quad (2)$$

where  $d_1$  and  $d_2$  denote the two deuterium nuclei of  $D_2^+$ . We remind the explicit form of the spin interaction operators; to comply with the established traditions we shall use atomic units  $\hbar = e = 4\pi\epsilon_0 = 1$  in the remainder of Sect. II A.

$$\begin{aligned} V_{ed_1} = \alpha^2 & \left[ -\frac{4\pi}{3} \mu_e \mu_d \frac{m_e}{m_p} \delta(\mathbf{r}_1) (\mathbf{s}_e \cdot \mathbf{I}_1) + \left( \mu_e - \frac{1}{2} \right) \frac{1}{r_1^3} (\mathbf{r}_1 \times \mathbf{p}_e) \cdot \mathbf{s}_e - \mu_e \frac{m_e}{m_d} \frac{1}{r_1^3} (\mathbf{r}_1 \times \mathbf{p}_1) \cdot \mathbf{s}_e \right. \\ & \left. - \frac{m_e}{2m_d} \left( \mu_d \frac{m_e}{m_p} - \frac{m_e}{m_d} \right) \frac{1}{r_1^3} (\mathbf{r}_1 \times \mathbf{p}_1) \cdot \mathbf{I}_1 + \mu_d \frac{m_e}{2m_p} \frac{1}{r_1^3} (\mathbf{r}_1 \times \mathbf{p}_e) \cdot \mathbf{I}_1 \right] \\ & + \alpha^2 \left[ \mu_e \mu_d \frac{m_e}{2m_p} \frac{r_1^2 (\mathbf{s}_e \cdot \mathbf{I}_1) - 3(\mathbf{r}_1 \cdot \mathbf{s}_e)(\mathbf{r}_1 \cdot \mathbf{I}_1)}{r_1^5} \right] + \frac{Q_d}{2a_0^2} \frac{r_1^2 \mathbf{I}_1^2 - 3(\mathbf{r}_1 \cdot \mathbf{I}_1)^2}{r_1^5}, \end{aligned} \quad (3)$$

$$V_{ed_2} = V_{ed_1}(\mathbf{r}_1 \rightarrow \mathbf{r}_2, \mathbf{p}_1 \rightarrow \mathbf{p}_2, \mathbf{I}_1 \rightarrow \mathbf{I}_2), \quad (4)$$

$$\begin{aligned} V_{dd} = \alpha^2 & \left[ -\frac{2\pi}{3} \mu_d^2 \frac{m_e^2}{m_p^2} \delta(\mathbf{r}_{12}) (\mathbf{I}_1 \cdot \mathbf{I}_2) + \frac{\mu_d m_e^2}{2m_p m_d} \left( \frac{1}{r_{12}^3} (\mathbf{r}_{12} \times \mathbf{p}_1) \cdot \mathbf{I}_2 - \frac{1}{r_{12}^3} (\mathbf{r}_{12} \times \mathbf{p}_2) \cdot \mathbf{I}_1 \right) \right. \\ & \left. + \frac{m_e}{2m_d} \left( \mu_d \frac{m_e}{m_p} - \frac{m_e}{m_d} \right) \left( \frac{1}{r_{12}^3} (\mathbf{r}_{12} \times \mathbf{p}_1) \cdot \mathbf{I}_1 - \frac{1}{r_{12}^3} (\mathbf{r}_{12} \times \mathbf{p}_2) \cdot \mathbf{I}_2 \right) \right] \\ & + \alpha^2 \left[ \mu_d^2 \frac{m_e^2}{4m_p^2} \frac{r_{12}^2 (\mathbf{I}_1 \cdot \mathbf{I}_2) - 3(\mathbf{r}_{12} \cdot \mathbf{I}_1)(\mathbf{r}_{12} \cdot \mathbf{I}_2)}{r_{12}^5} \right] - \frac{Q_d}{2a_0^2} \sum_{i=1,2} \frac{r_{12}^2 \mathbf{I}_i^2 - 3(\mathbf{r}_{12} \cdot \mathbf{I}_i)^2}{r_{12}^5}. \end{aligned} \quad (5)$$

Here  $\mathbf{I}_{1,2}$  and  $\mathbf{s}_e$  are the spin operators of the two deuterons and of the electron, respectively, and proper symmetrization of the terms containing non-commuting operators is assumed;  $\mu_e$  is the magnetic dipole moment of the electron in units  $\mu_0 = e\hbar/2m_e$  (Bohr magneton),  $\mu_d$  is the magnetic dipole moment of the deuteron in units  $\mu_N = e\hbar/2m_p$  (nuclear magneton),  $a_0$  is the Bohr radius, and  $Q_d$  is the electric quadrupole moment of the deuteron. The same spin-interaction Hamiltonian was used in [11].

The spin interactions split the degenerate nonrelativistic energy levels  $E^{(\text{NR})vL}$  into a manifold of hyperfine levels that are distinguished with additional quantum numbers (QNs) describing their ‘‘spin composition’’. As evidenced in subsection II C, the appropriate angular momentum coupling scheme for  $D_2^+$  is

$$\mathbf{I} = \mathbf{I}_1 + \mathbf{I}_2, \quad \mathbf{F} = \mathbf{I} + \mathbf{s}_e, \quad \mathbf{J} = \mathbf{L} + \mathbf{F}.$$

Accordingly, the hyperfine states are labelled with the exact QNs of the total angular momentum  $J$  and its projection  $J_z$ , and the approximate QNs  $I$ ,  $F$  and  $L$ . Similar to Refs. [10, 11, 14], in first order of perturbation theory the hyperfine levels  $E^{(vL)IFJJ_z}$  are put in the form

$$E^{(vL)IFJJ_z} = E^{(\text{NR})vL} + \Delta E^{(vL)IFJJ_z}, \quad (6)$$

where the corrections  $\Delta E^{(vL)IFJJ_z}$ , also referred to as ‘hyperfine energies’ or ‘hyperfine shifts’, are the eigenvalues of the effective spin interaction Hamiltonian  $H^{\text{eff}}$ . (Of course, in absence of external fields the energies are degenerate in  $J_z$ ). Since this is the point where our results disagree to some extent with the results of Refs. [11, 12], we give more details of the calculations.

## B. Effective spin Hamiltonian

We associate with the spin of the deuteron  $d_1$  the  $(2I_1 + 1)$ -dimensional space of the irreducible representation ( $I_1$ ) of  $su(2)$  with basis vectors  $|I_1 I_{1z}\rangle$ ,  $I_{1z} = -I_1, \dots, I_1$ , satisfying

$$\hat{I}_1^2 |I_1 I_{1z}\rangle = I_1(I_1 + 1) |I_1 I_{1z}\rangle, \quad \hat{I}_{1z} |I_1 I_{1z}\rangle = I_{1z} |I_1 I_{1z}\rangle.$$

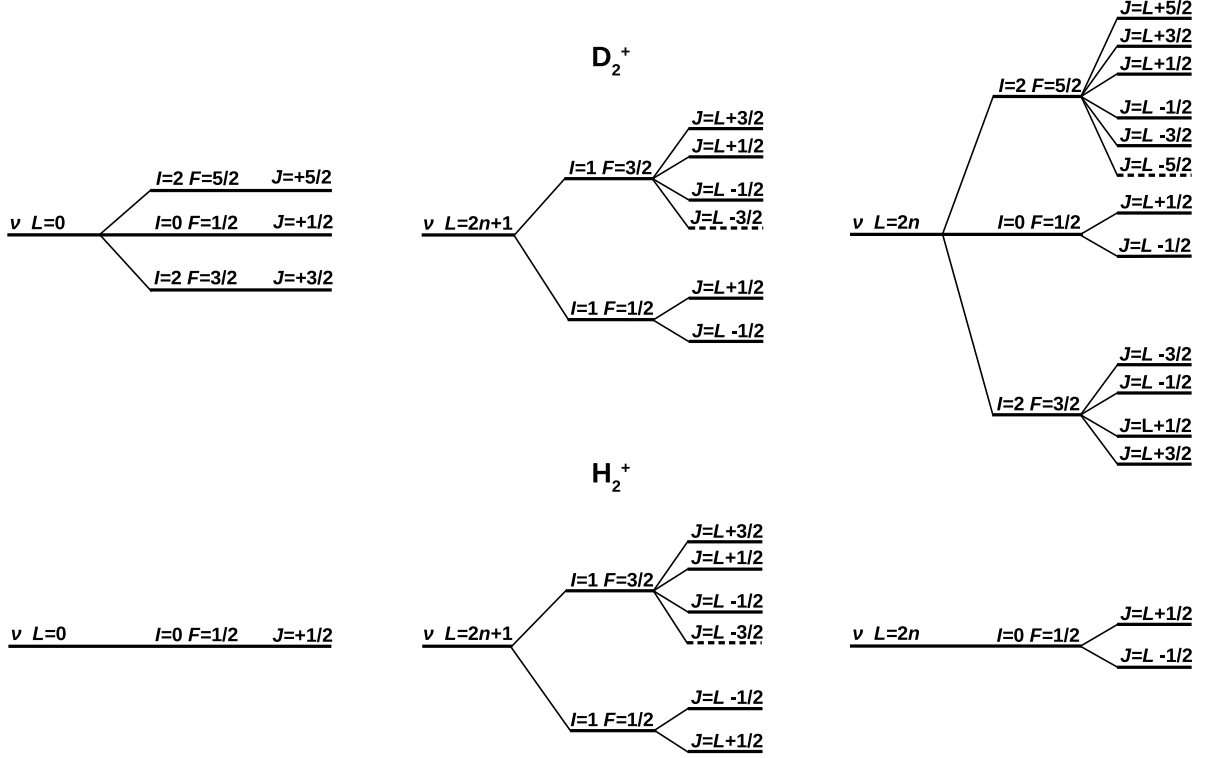


FIG. 1: Comparison of the hyperfine structure of the molecular ions  $D_2^+$  and  $H_2^+$ , for even  $L = 2n, n = 1, 2, \dots$  and odd  $L = 2n + 1, n = 0, 1, \dots$  values of  $L$  and for  $L=0$ . For  $1 \leq L \leq 2$  the states marked with dashed lines do not exist (see Tables III,IV). For  $L=0$  the HFS of  $D_2^+$  consists of only three states; similar to  $H_2^+$  the one with  $I=0$  has no hyperfine shift.

Similarly, we define the sets  $|I_2 I_{2z}\rangle$ ,  $|s_e s_{ez}\rangle$ , and  $|LL_z\rangle$ . The basis set  $|IFF_z\rangle$  in the resulting space of the spin variables of all  $D_2^+$  constituents is taken in the form:

$$|IFF_z\rangle = \sum_{I_{1z} I_{2z} s_{ez} I_z} C_{I_1 I_{1z}, I_2 I_{2z}}^{II_z} C_{II_z, s_e s_{ez}}^{FF_z} |I_1 I_{1z}\rangle |I_2 I_{2z}\rangle |s_e s_{ez}\rangle, \quad (7)$$

here  $C_{l_1 m_1, l_2 m_2}^{LM} = \langle l_1 l_2 m_1 m_2 | LM \rangle$  are Clebsch-Gordan coefficients. Thus, the basis set in the hyperfine manifold of the  $(vL)$  state of  $D_2^+$  consists of the functions

$$\Psi_0^{(vL)IFJJ_z} = \sum_{L_z F_z} C_{LL_z, FF_z}^{JJ_z} \Psi^{(\text{NR})vLL_z} |IFF_z\rangle. \quad (8)$$

We also define a basis set depending on the angular part only, which will be referred to as "pure" states,

$$|LIFJJ_z\rangle = \sum_{L_z, F_z} C_{LL_z, FF_z}^{JJ_z} |LL_z\rangle |IFF_z\rangle. \quad (9)$$

The effective spin Hamiltonian  $H^{\text{eff}}$  is a matrix operator acting on the finite-dimensional space spanned by the vectors  $|LIFJJ_z\rangle$ , such that

$$H_{I'F',IF}^{\text{eff}(vL)J} \equiv \langle LI'F'JJ_z | H^{\text{eff}} |LIFJJ_z\rangle = \langle \Psi_0^{(vL)I'F'JJ_z} | V | \Psi_0^{(vL)IFJJ_z} \rangle. \quad (10)$$

$I$	$F$	$J$	This work	[11]	[13]
$(vL) = (01)$					
1	3/2	5/2	80.6242	80.623(4)	80.597
1	3/2	1/2	70.3510	70.355(4)	70.319
1	3/2	1/2	47.9162	47.910(3)	47.878
1	1/2	1/2	-136.4929	-136.492(7)	-136.436
1	1/2	3/2	-146.9989	-146.999(8)	-146.94

TABLE I: Comparison of the hyperfine energies  $\Delta E^{(vL)IFJ}$  for the  $(vL) = (01)$  state, in MHz, calculated in the present work and in Refs. [11] and [13]. The fractional uncertainty of the results of the present work and [11, 12] is estimated as  $O(\alpha^2)$ .

In absence of external fields the matrix of  $H_{I'F',IF}^{\text{eff}(vL)J}$  is independent of  $J_z$ . For the deuterium molecular ion  $H^{\text{eff}}$  has the form

$$\begin{aligned}
H^{\text{eff}} = & E_1(\mathbf{L} \cdot \mathbf{s}_e) + E_2(\mathbf{L} \cdot \mathbf{I}) + E_3(\mathbf{I} \cdot \mathbf{s}_e) \\
& + E_4(2\mathbf{L}^2(\mathbf{I} \cdot \mathbf{s}_e) - 3((\mathbf{L} \cdot \mathbf{I})(\mathbf{L} \cdot \mathbf{s}_e) + (\mathbf{L} \cdot \mathbf{s}_e)(\mathbf{L} \cdot \mathbf{I}))) \\
& + E_5(2\mathbf{L}^2(\mathbf{I}_1 \cdot \mathbf{I}_2) - 3((\mathbf{L} \cdot \mathbf{I}_1)(\mathbf{L} \cdot \mathbf{I}_2) + (\mathbf{L} \cdot \mathbf{I}_2)(\mathbf{L} \cdot \mathbf{I}_1))) \\
& + E_6 \left[ \mathbf{L}^2 \mathbf{I}_1^2 - \frac{3}{2}(\mathbf{L} \cdot \mathbf{I}_1) - 3(\mathbf{L} \cdot \mathbf{I}_1)^2 + \mathbf{L}^2 \mathbf{I}_2^2 - \frac{3}{2}(\mathbf{L} \cdot \mathbf{I}_2) - 3(\mathbf{L} \cdot \mathbf{I}_2)^2 \right].
\end{aligned} \tag{11}$$

Compared to the effective spin Hamiltonian for  $\text{H}_2^+$  of Ref. [10],  $H^{\text{eff}}$  of Eq. (11) includes one additional term (with  $E_6$ , last line) that describes the effects due to the electric quadrupole moment of the nuclei and arises when averaging the last term in Eqs. (3-5). The first four terms in Eq. (11) coincide with the first four terms in the effective Hamiltonian of Refs. [11, 12], defined in Eqs. (12)-(15) of the former, with account of the correspondence between the notations used:  $E_1 = c_e$ ,  $E_2 = c_I$ ,  $E_3 = b_F$ ,  $E_4 = d_1/(3(2L-1)(2L+3))$ . The last two terms involving  $E_5$  and  $E_6$ , however, do not. The disagreement appears in the terms related to the tensor interaction of the deuterons in the last lines of Eqs. (3) and (5). The explicit expressions for  $E_4$ - $E_6$  are:

$$\begin{aligned}
E_4 = & \alpha^2 \mu_e \mu_d \frac{m_e}{2m_p} \left[ \frac{\langle vL \| r_1^{-5} (\mathbf{r}_1^2 \delta_{ij} - 3r_{1i} r_{1j}) \| vL \rangle}{\langle L \| 2\mathbf{L}^2 \delta_{ij} - 3(L_i L_j + L_j L_i) \| L \rangle} + (1 \rightarrow 2) \right], \\
E_5 = & \alpha^2 \left( \frac{\mu_d m_e}{2m_p} \right)^2 \frac{\langle vL \| r_{12}^{-5} (\delta_{ij} \mathbf{r}_{12}^2 - 3r_{12i} r_{12j}) \| vL \rangle}{\langle L \| 2\mathbf{L}^2 \delta_{ij} - 3(L_i L_j + L_j L_i) \| L \rangle}, \\
E_6 = & \frac{Q_d}{2} \left[ \frac{\langle vL \| r_1^{-5} (\delta_{ij} \mathbf{r}_1^2 - 3r_i r_j) \| vL \rangle - \langle vL \| r_{12}^{-5} (\delta_{ij} \mathbf{r}_{12}^2 - 3r_{12i} r_{12j}) \| vL \rangle}{\langle L \| \mathbf{L}^2 \delta_{ij} - (3/2)(L_i L_j + L_j L_i) \| L \rangle} + (1 \rightarrow 2) \right],
\end{aligned} \tag{12}$$

where  $\langle v'L' \| \dots \| vL \rangle$  denote reduced matrix elements in the basis of nonrelativistic wave functions  $\psi^{(\text{NR})vLLz}$ , while

$$\langle L \| 2\mathbf{L}^2 \delta_{ij} - 3(L_i L_j + L_j L_i) \| L \rangle = -2\sqrt{L(L+1)}\sqrt{(2L-1)(2L+1)(2L+3)}.$$

is a reduced matrix element in the basis of the representation  $(L)$  of  $su(2)$  (see Eqs. (7),(9)). The three coefficients depend on two spatial integrals and thus may be easily related to each other. To complete the comparison with [11] we also mention that the second-order tensors in the last two lines of Eq. (11) cannot be reduced to the form used in Eq. (10) of Ref. [11]. The effective Hamiltonian of [11] does not connect the states with  $I = 0$  and 2, while the last two terms in Eq. (11) have nonzero matrix elements connecting the "pure state" vectors of Eq. (9) with different total nuclear spin.

In first order of perturbation theory the wave functions of  $\text{D}_2^+$  are linear combinations of the basis set (8):

$$\Psi^{(vL)IFJJ_z} = \sum_{I'F'} \beta_{I'F'}^{(vL)IFJ} \Psi_0^{(vL)I'F'JJ_z}, \tag{13}$$

where the constant amplitudes  $\beta_{I'F'}^{(vL)IFJ}$  and the hyperfine shifts  $\Delta E^{(vL)IFJ}$  are the eigenvectors and eigenvalues of the matrix of  $H^{\text{eff}}$  in the basis of pure states (9):

$$\sum_{I''F''} H_{I'F',I''F''}^{\text{eff}(vL)J} \beta_{I''F''}^{(vL)IFJ} = \Delta E^{(vL)IFJ} \beta_{I'F'}^{(vL)IFJ}. \tag{14}$$

Similar to  $\text{H}_2^+$ , symmetry with respect to exchange of the identical nuclei imposes restrictions on the allowed values of  $I$  in the summation in Eqs. (13), (14); for  $\Sigma_g$  states, in particular,  $I$  must satisfy  $(-1)^{L+I} = 1$ . As a result, in  $\text{H}_2^+$ , in first order of perturbation theory,  $I$  turns out to be an exact quantum number [10]. This is not the case for  $\text{D}_2^+$ , however, where both values  $I = 0$  and  $I = 2$  are allowed for even values of  $L$ , although their mixing is weak. Still, a few of the hyperfine states of  $\text{D}_2^+$  are “pure states” with no mixing and all quantum numbers *exact*; these are the states with  $I = 1$ ,  $F = 3/2$ ,  $J = L \pm F$  (for odd  $L$ ), the states with  $I = 2$ ,  $F = 5/2$ ,  $J = L \pm F$  (for even  $L \geq 2$ ), as well as the states with  $L = 0$  and either  $I = 0, J = F = 1/2$  or  $I = 2, J = F = I \pm 1/2$ . The “stretched” states with  $F = I + 1/2$ ,  $J = L + F$ , and  $J_z = \pm J$ , of significant experimental interest because their Zeeman shift is strictly linear in the magnetic shift in first order of perturbation theory [15], are a sub-class of the “pure” states listed above. The hyperfine energy  $\Delta E \equiv \Delta E^{(vL)IFJ}$  of the “pure” states is simply expressed in terms of the coefficients of the effective spin Hamiltonian as follows:

$$\begin{aligned} \Delta E^{(vL)IFJ} &= \frac{1}{2}(E_3 + L(E_1 + 2E_2 + (2L - 1)(E_6 - 2E_4 - 2E_5))), \text{ for } I = 1, F = 3/2, J = L + F, \text{ odd } L; \\ \Delta E^{(vL)IFJ} &= \frac{1}{2}(E_3 - (L + 1)(E_1 + 2E_2 + (2L + 3)(E_6 - 2E_4 - 2E_5))), \text{ for } I = 1, F = 3/2, J = L - F, \text{ odd } L \geq 3; \\ \Delta E^{(vL)IFJ} &= E_3 + L(E_1/2 + 2E_2 - (2L - 1)(2E_4 + 2E_5 + E_6)), \text{ for } I = 2, F = 5/2, J = L + F, \text{ even } L \geq 2; \\ \Delta E^{(vL)IFJ} &= E_3 - (L + 1)(E_1/2 + 2E_2 + (2L + 3)(2E_4 + 2E_5 + E_6)), \text{ for } I = 2, F = 5/2, J = L - F, \text{ even } L \geq 4; \\ \Delta E^{(v0)0FJ} &= 0 \text{ for } J = F = 1/2, \\ \Delta E^{(v0)2FJ} &= -3E_3/2 \text{ for } J = F = 3/2, \\ \Delta E^{(v0)2FJ} &= E_3 \text{ for } J = F = 5/2. \end{aligned}$$

### C. Numerical results

The numerical results of the present work were obtained using the non-relativistic wave functions  $\Psi^{(\text{NR})vLLz}$  of  $\text{D}_2^+$ , calculated with high numerical precision in the variational approach of Ref. [16]. Throughout the calculations the CODATA18 values [17] of fundamental constants were used for  $m_d/m_p$ ,  $\mu_e$ , and  $\mu_d$ , while  $Q_d = 0.285783 \text{ fm}^2$  was taken from [18]. Table II gives the values of  $E_n, n = 1, \dots, 6$  for the lower ro-vibrational states of  $\text{D}_2^+$ ; the values for all ro-vibrational states  $(vL)$  with  $v \leq 10$  and  $L \leq 4$  can be found in the electronic supplement. The theoretical uncertainty of  $E_n$  is due to the neglected contribution from QED and relativistic effects of order  $O(m_e\alpha^6)$  and higher that are not accounted for by the Breit-Pauli Hamiltonian and is estimated to be fractionally of order  $O(\alpha^2) \sim 0.5 \times 10^{-4}$ ; the numerical uncertainty related to numerical integration etc. is smaller. In Table II we list the numerical values of  $E_n, n = 1, \dots, 6$  with 6 significant digits to avoid rounding errors in further calculations.

The hyperfine energies  $\Delta E^{(vL)IFJ}$  and the amplitudes  $\beta_{IF'}^{(vL)IFJ}$  of the states from the hyperfine structure of the lower excited states, calculated using Eqs. (10), (11), and (14), are given in Tables III and IV. The results for the higher excited states with  $v$  up to 10 or  $L$  up to 4 are available in the electronic supplement.

In the lower ro-vibrational states of  $\text{D}_2^+$  the dominating term of the Breit-Pauli Hamiltonian (3-5) is the contact spin-spin interaction between the electron and the nuclei; this can be recognized by comparing the value of  $E_3$  with the other coefficients of the effective spin Hamiltonian  $H^{\text{eff}}$  (11), given in Table II and the electronic supplement. The contribution to  $\Delta E^{(vL)IFJ}$  of the  $E_3$ -term alone is  $(E_3/2)(F(F+1) - I(I+1) - 3/4)$ ; similar to  $\text{H}_2^+$  it qualitatively determines the shape of the hyperfine level structure (see Fig. 1), and for  $L = 0$  this is the only contribution to the hyperfine energy. The typical separation between hyperfine levels of  $\text{D}_2^+$  with different values of  $F$  or  $I$  is of the order of  $E_3 \sim 10^2$  MHz. It is significantly smaller than the GHz separation in  $\text{H}_2^+$  or  $\text{HD}^+$  because of the smaller magnetic dipole moment of the deuteron  $\mu_d$  as compared with  $\mu_p$ . For all three molecular ions the separation between states with  $\Delta J = \pm 1$  is of the order of 10 MHz.

The fractional uncertainty of  $\Delta E^{(vL)IFJ}$  is estimated to be of fractional order  $O(\alpha^2) \simeq 0.5 \times 10^{-4}$ , same as for the coefficients  $E_n$  of  $H^{\text{eff}}$ . For hyperfine states with shifts of the order of 100 MHz the theoretical uncertainty amounts to the order of 5 kHz. For states with the smallest shifts ( $\simeq 20$  MHz, in which the influence of the coefficient  $E_3$  is comparatively small), the uncertainties are of order 1 kHz.

Comparison of our results for  $\Delta E^{(vL)IFJ}$  with the results of Ref. [11] shows that for the majority of the considered hyperfine states the difference is within  $\alpha^2 |\Delta E^{(vL)IFJ}|$ , although for a number of cases (e.g. the state  $(vLIFJ) = (011\frac{3}{2}\frac{1}{2})$ , see Table I) it exceeds the uncertainty explicitly indicated in [11]. We attribute this to the incorrect form of the effective spin Hamiltonian used in [11].

Zhang et al. [11] and earlier Babb [23] raised the interesting question about the possibility of determining  $Q_d$  from the hyperfine structure of  $\text{D}_2^+$ ; there is now an intense discussion on its actual value. Recently, Alighanbari et

$v$	$L$	$E_1$	$E_2$	$E_3$	$E_4$	$E_5$	$E_6$
0	0			142.533			
1	0			139.837			
2	0			137.286			
3	0			134.873			
4	0			132.593			
0	1	21.4599	-3.21518[-3]	142.448	1.32980	-4.71443[-4]	5.67068[-3]
1	1	20.5231	-3.12947[-3]	139.756	1.26978	-4.57403[-4]	5.66924[-3]
2	1	19.6183	-3.04185[-3]	137.209	1.21191	-4.43279[-4]	5.64719[-3]
3	1	18.7423	-2.95244[-3]	134.799	1.15600	-4.29061[-4]	5.60575[-3]
4	1	17.8923	-2.86128[-3]	132.522	1.10187	-4.14738[-4]	5.54600[-3]
0	2	21.3955	-3.20207[-3]	142.278	3.15886[-1]	-1.11799[-4]	1.34038[-3]
1	2	20.4612	-3.11645[-3]	139.594	3.01623[-1]	-1.08462[-4]	1.34003[-3]
2	2	19.5586	-3.02901[-3]	137.054	2.87871[-1]	-1.05106[-4]	1.33480[-3]
3	2	18.6847	-2.93977[-3]	134.652	2.74583[-1]	-1.01728[-4]	1.32498[-3]
4	2	17.8368	-2.84875[-3]	132.382	2.61720[-1]	-9.83254[-5]	1.31082[-3]
0	3	21.2995	-3.18256[-3]	142.025	1.46902[-1]	-5.18607[-5]	6.18729[-4]
1	3	20.3688	-3.09714[-3]	139.353	1.40266[-1]	-5.03083[-5]	6.18561[-4]
2	3	19.4696	-3.00991[-3]	136.824	1.33867[-1]	-4.87468[-5]	6.16135[-4]
3	3	18.5989	-2.92092[-3]	134.432	1.27684[-1]	-4.71753[-5]	6.11585[-4]
4	3	17.7541	-2.83015[-3]	132.173	1.21697[-1]	-4.55926[-5]	6.05027[-4]
0	4	21.1727	-3.15685[-3]	141.691	8.54566[-2]	-3.00678[-5]	3.56385[-4]
1	4	20.2467	-3.07169[-3]	139.033	8.15938[-2]	-2.91641[-5]	3.56285[-4]
2	4	19.3519	-2.98476[-3]	136.519	7.78684[-2]	-2.82552[-5]	3.54880[-4]
3	4	18.4855	-2.89608[-3]	134.142	7.42682[-2]	-2.73407[-5]	3.52246[-4]
4	4	17.6446	-2.80567[-3]	131.896	7.07820[-2]	-2.64197[-5]	3.48452[-4]

TABLE II: Coefficients of the effective spin interaction Hamiltonian of Eq. (11) for the lower ro-vibrational states of  $D_2^+$  with  $L \leq 4$ ,  $v \leq 10$ , in MHz. The number in brackets denote powers of ten:  $a[b] = a \times 10^b$ . Note that for  $L = 0$  all coefficients but  $E_3$  are zero.

al. [22] determined  $Q_d$  with an uncertainty of 1.5 % from the hyperfine spectrum of a pure rotational transition of  $HD^+$ . However, the most precise determination so far is from a comparison of experiment and theory for the neutral hydrogen molecules [18–20]. Their stated uncertainties, ranging from  $1 \times 10^{-4}$  to  $8 \times 10^{-4}$ , are so small that it is worthwhile to perform an independent measurement, using the molecular hydrogen ion  $HD^+$  or  $D_2^+$ .

As a matter of principle, the determination of  $Q_d$  with  $D_2^+$  can only reach a fractional uncertainty equal to the fractional uncertainty of the relevant coefficient  $E_6$ . Here, we have calculated it to a fractional uncertainty of order  $\alpha^2$ , as was done for the relevant coefficient  $E_9$  for  $HD^+$ . The use of the variational non-relativistic wave functions of  $D_2^+$  [16] eliminates the uncertainties from neglected non-adiabatic effects and therefore already represents an important and necessary step towards a new determination of  $Q_d$ .

In the future, a calculation of the coefficients of  $H^{\text{eff}}$  could be performed by taking into account the QED corrections of order  $O(m_e \alpha^6)$  and higher, as was already performed for  $H_2^+$  [10]. This would represent a further significant step.

Furthermore, we show in the rightmost column of Tables III and IV the (numerically calculated) derivatives of the hyperfine energies with respect to the electric quadrupole moment of the deuteron  $Q_d$ . Note that while the coefficient  $E_6$  decreases substantially when  $L$  goes from 1 to 3, the largest sensitivities among the hyperfine states actually slightly increase. Relevant for the determination of  $Q_d$  are the differences of the sensitivities of upper and lower state of a transition. Some of these are given in Table VI. It can be seen from the largest differences ( $\simeq 100 \text{ kHz fm}^{-2}$ ) that the experimental and theoretical uncertainties have to be on the order 3 Hz or less, in order to match the present uncertainty of  $Q_d$ .

However, an additional issue is the theoretical uncertainty of the dominant hyperfine hamiltonian coefficients  $E_1, E_3, E_4$ . As mentioned above, it can lead to absolute uncertainties of the order of 2 kHz for certain favorable hyperfine transition components, i.e. comparable to  $E_6$  itself, and significantly more for others. An approach to overcome these uncertainties, at least to a certain degree, has been implemented in Ref. [22].

Note that the off-diagonal elements of the matrix  $\beta_{I'F'}^{IFJ}$  (see Eq. (13)) are small, i.e. the mixing of states with different values of  $I$  or  $F$  is weak. This justifies our choice of the angular momentum coupling scheme, and allows to use in estimates of the characteristics of  $D_2^+$  (except for the hyperfine shifts) the approximation of pure states  $\beta_{I'F'}^{IFJ} = \delta_{F'F} \delta_{I'I}$ . In calculations of the hyperfine energies a neglect of the  $F$ -mixing induces a fractional error of the order of half of a percent while the  $I$ -mixing contributes below the level of  $10^{-8}$  and is of no practical importance.

$I$	$F$	$J$	$\Delta E^{\text{hfs}}/h$	$\beta_{1,1/2}^{IFJ}$	$\beta_{1,3/2}^{IFJ}$	$(d\Delta E^{\text{hfs}}/dQ_d)/h$
$v = 0, L = 1$						
1	1/2	3/2	-146.999	0.99776	-0.06688	2.78
1	1/2	1/2	-136.493	0.99673	-0.08075	-10.97
1	3/2	1/2	47.916	0.08075	0.99673	60.58
1	3/2	3/2	70.351	0.06688	0.99776	-42.47
<b>1</b>	<b>3/2</b>	<b>5/2</b>	<b>80.624</b>	<b>0.00000</b>	<b>1.00000</b>	<b>9.92</b>
$v = 1, L = 1$						
1	1/2	3/2	-144.085	0.99787	-0.06524	2.72
1	1/2	1/2	-134.026	0.99692	-0.07838	-10.66
1	3/2	1/2	47.564	0.07838	0.99692	60.25
1	3/2	3/2	69.012	0.06524	0.99787	-42.39
<b>1</b>	<b>3/2</b>	<b>5/2</b>	<b>78.870</b>	<b>0.00000</b>	<b>1.00000</b>	<b>9.92</b>
$v = 2, L = 1$						
1	1/2	3/2	-141.325	0.99798	-0.06356	2.64
1	1/2	1/2	-131.698	0.99711	-0.07598	-10.30
1	3/2	1/2	47.251	0.07598	0.99711	59.70
1	3/2	3/2	67.746	0.06356	0.99798	-42.16
<b>1</b>	<b>3/2</b>	<b>5/2</b>	<b>77.202</b>	<b>0.00000</b>	<b>1.00000</b>	<b>9.88</b>
$v = 0, L = 3$						
1	1/2	7/2	-157.925	0.98895	-0.14826	7.53
1	1/2	5/2	-134.446	0.98227	-0.18749	-16.39
<b>1</b>	<b>3/2</b>	<b>3/2</b>	<b>23.151</b>	<b>0.00000</b>	<b>1.00000</b>	<b>3.87</b>
1	3/2	5/2	54.118	0.18749	0.98227	6.65
1	3/2	7/2	80.653	0.14826	0.98895	-40.01
<b>1</b>	<b>3/2</b>	<b>9/2</b>	<b>100.754</b>	<b>0.00000</b>	<b>1.00000</b>	<b>16.24</b>
$v = 1, L = 3$						
1	1/2	7/2	-154.445	0.98944	-0.14497	7.38
1	1/2	5/2	-131.922	0.98324	-0.18230	-15.94
<b>1</b>	<b>3/2</b>	<b>3/2</b>	<b>23.914</b>	<b>0.00000</b>	<b>1.00000</b>	<b>38.96</b>
1	3/2	5/2	53.336	0.18230	0.98324	6.20
1	3/2	7/2	78.775	0.14497	0.98944	-39.85
<b>1</b>	<b>3/2</b>	<b>9/2</b>	<b>98.122</b>	<b>0.00000</b>	<b>1.00000</b>	<b>16.23</b>
$v = 2, L = 3$						
1	1/2	7/2	-151.139	0.98992	-0.14161	7.20
1	1/2	5/2	-129.544	0.98421	-0.17702	-15.42
1	3/2	3/2	24.678	0.00000	1.00000	38.81
1	3/2	5/2	52.614	0.17702	0.98421	5.72
1	3/2	7/2	76.992	0.14161	0.98992	-39.54
1	3/2	9/2	95.605	0.00000	1.00000	16.17

TABLE III: Hyperfine structure of the lower ro-vibrational states for odd values  $L = 1, 3$ . Listed are: the quantum numbers  $J$ ,  $I$ , and  $F$ , the hyperfine energy  $\Delta E^{\text{hfs}} = \Delta E^{(vL)IFJ}/h$  (in MHz), the amplitudes  $\beta_{I'F'}^{(vL)IFJ}$  of the spin wave function, and the derivative  $h^{-1} d\Delta E^{\text{hfs}}/dQ_d$  (in kHz fm $^{-2}$ ). The stretched states are typed in boldface.

### III. ELECTRIC QUADRUPOLE TRANSITIONS

#### A. Hyperfine structure of the $E2$ spectra in homonuclear molecular ions

The evaluation of the electric quadrupole transition spectrum of  $D_2^+$  follows closely the procedure described in details in [10]; we shall highlight the points that are specific for the  $D_2^+$  molecule, and also take the opportunity to refine some of the definitions given there. The use of dimensional SI units is restored in the rest of the paper.

Similar to Eqs. (5)-(7) of [10], we denote by  $H_{\text{int}}^{(E2)}$  the terms in the interaction Hamiltonian of  $D_2^+$  with a monochromatic electromagnetic plane wave, which are responsible for the electric quadrupole transitions. We take the vector potential in the form  $\mathbf{A}(\mathbf{R}, t) = (-i/\omega) (\mathbf{E}_0 e^{i(\mathbf{k}\cdot\mathbf{R}-\omega t)} - \mathbf{E}_0^* e^{-i(\mathbf{k}\cdot\mathbf{R}-\omega t)})$ , where  $\mathbf{k}$  is the wave vector,  $\omega = c|\mathbf{k}|$  is the circular frequency, and  $\mathbf{E}_0$  – the amplitude of the oscillating electric field,

The  $E2$  transition matrix element between the initial  $|i\rangle = |(vL)IFJJ_z\rangle$  and final  $|f\rangle = |(v'L')I'F'J'J'_z\rangle$  hyperfine

$I$	$F$	$J$	$\Delta E^{\text{hfs}}/h$	$\beta_{0,1/2}^{IFJ}$	$\beta_{2,3/2}^{IFJ}$	$\beta_{2,5/2}^{IFJ}$	$(d\Delta E^{\text{hfs}}/dQ_d)/h$
$v = 0, L = 0$							
<b>2</b>	<b>3/2</b>	<b>3/2</b>	<b>-213.800</b>	<b>0.00000</b>	<b>1.00000</b>	<b>0.00000</b>	<b>0.00000</b>
<b>0</b>	<b>1/2</b>	<b>1/2</b>	<b>0.000</b>	<b>1.00000</b>	<b>0.00000</b>	<b>0.00000</b>	<b>0.00000</b>
<b>2</b>	<b>5/2</b>	<b>5/2</b>	<b>142.533</b>	<b>0.00000</b>	<b>0.00000</b>	<b>1.00000</b>	<b>0.00000</b>
$v = 1, L = 0$							
<b>2</b>	<b>3/2</b>	<b>3/2</b>	<b>-209.756</b>	<b>0.00000</b>	<b>1.00000</b>	<b>0.00000</b>	<b>0.00000</b>
<b>0</b>	<b>1/2</b>	<b>1/2</b>	<b>0.000</b>	<b>1.00000</b>	<b>0.00000</b>	<b>0.00000</b>	<b>0.00000</b>
<b>2</b>	<b>5/2</b>	<b>5/2</b>	<b>139.837</b>	<b>0.00000</b>	<b>0.00000</b>	<b>1.00000</b>	<b>0.00000</b>
$v = 0, L = 2$							
2	3/2	7/2	-226.255	0.00000	0.99852	-0.05446	-22.25
2	3/2	5/2	-216.433	0.00004	0.99669	-0.08128	51.39
2	3/2	3/2	-202.716	-0.00012	0.99664	-0.08194	5.06
2	3/2	1/2	-190.986	0.00000	0.99863	-0.05238	-66.45
0	1/2	3/2	-32.093	1.00000	0.00012	0.00006	0.01
0	1/2	5/2	21.395	1.00000	-0.00002	0.00019	-0.02
2	5/2	1/2	102.515	0.00000	0.05238	0.99863	-81.29
2	5/2	3/2	117.107	-0.00007	0.08194	0.99664	-33.21
2	5/2	5/2	135.572	-0.00019	0.08128	0.99669	26.03
2	5/2	7/2	151.994	0.00000	0.05446	0.99852	50.39
<b>2</b>	<b>5/2</b>	<b>9/2</b>	<b>159.864</b>	<b>0.00000</b>	<b>0.00000</b>	<b>1.00000</b>	<b>-28.14</b>
$v = 1, L = 2$							
2	3/2	7/2	-221.646	0.00000	0.99858	-0.05318	-22.19
2	3/2	5/2	-212.213	0.00004	0.99686	-0.07921	51.32
2	3/2	3/2	-199.097	-0.00012	0.99682	-0.07963	4.92
2	3/2	1/2	-187.921	0.00000	0.99871	-0.05076	-66.51
0	1/2	3/2	-30.692	1.00000	0.00013	0.00007	0.01
0	1/2	5/2	20.461	1.00000	-0.00002	0.00019	-0.02
2	5/2	1/2	101.558	0.00000	0.05076	0.99871	-81.19
2	5/2	3/2	115.469	-0.00008	0.07963	0.99682	-33.07
2	5/2	5/2	133.118	-0.00019	0.07921	0.99686	26.07
2	5/2	7/2	148.851	0.00000	0.05318	0.99858	50.33
<b>2</b>	<b>5/2</b>	<b>9/2</b>	<b>156.416</b>	<b>0.00000</b>	<b>0.00000</b>	<b>1.00000</b>	<b>-28.13</b>
$v = 2, L = 2$							
2	3/2	7/2	-217.273	0.00000	0.99865	-0.05189	-22.05
2	3/2	5/2	-208.218	0.00004	0.99702	-0.07710	51.07
2	3/2	3/2	-195.684	-0.00012	0.99701	-0.07728	4.76
2	3/2	1/2	-185.041	0.00000	0.99879	-0.04913	-6.63
0	1/2	3/2	-29.338	1.00000	0.00013	0.00007	0.01
0	1/2	5/2	19.559	1.00000	-0.00002	0.00019	-0.02
2	5/2	1/2	100.687	0.00000	0.04913	0.99879	80.80
2	5/2	3/2	113.941	-0.00008	0.07728	0.99701	-32.80
2	5/2	5/2	130.803	-0.00019	0.07710	0.99702	26.02
2	5/2	7/2	145.870	0.00000	0.05189	0.99865	50.07
<b>2</b>	<b>5/2</b>	<b>9/2</b>	<b>153.139</b>	<b>0.00000</b>	<b>0.00000</b>	<b>1.00000</b>	<b>-28.02</b>

TABLE IV: Hyperfine structure of the lower ro-vibrational states for even values  $L=0, 2$ . Listed are: the quantum numbers  $J$ ,  $I$ , and  $F$ , the hyperfine energy  $\Delta E^{\text{hfs}} = \Delta E^{(vL)IFJ}/h$  (in MHz), the amplitudes  $\beta_{I',F'}^{(vL)IFJ}$  of the spin wave function, and the derivative  $h^{-1} d\Delta E^{\text{hfs}}/dQ_d$  (in kHz fm $^{-2}$ ). The stretched states are typed in boldface. Note that the values of  $\beta_{0,1/2}^{IFJ}$ ,  $I=0$ ,  $F=1/2$ ,  $L=2$  are strictly less than 1 but appear as 1.00000 due to rounding to 5 significant digits. On the contrary,  $\Delta E^{\text{hfs}}$  for  $I=0$ ,  $F=J=1/2$  is strictly zero.

states of  $D_2^+$  is

$$\begin{aligned}
\langle \Psi^{(v'L')I'F'J'J'_z} | H_{\text{int}}^{(E2)} | \Psi^{(vL)IFJJ_z} \rangle &= \frac{i}{3c} \omega^{\text{NR}} | \mathbf{E}_0 | \times \\
&\left( e^{-i\omega t} \langle \Psi^{(v'L')I'F'J'J'_z} | \hat{T}_{ij}^{(2)} Q_{ij}^{(2)} | \Psi^{(vL)IFJJ_z} \rangle + e^{i\omega t} \langle \Psi^{(v'L')I'F'J'J'_z} | \hat{T}_{ij}^{(2)*} Q_{ij}^{(2)} | \Psi^{(vL)IFJJ_z} \rangle \right),
\end{aligned} \tag{15}$$

where  $\omega^{\text{NR}} = (E^{(\text{NR})v'L'} - E^{(\text{NR})vL})/\hbar$  is the transition circular frequency in the non-relativistic approximation, the



asterisk denotes complex conjugation, and the tensor of the electric quadrupole transition operator is defined as

$$Q_{ij}^{(2)} = \frac{1}{2} \sum_{\alpha} Z_{\alpha} e (3R_{\alpha i} R_{\alpha j} - \delta_{ij} \mathbf{R}_{\alpha}^2), \quad (16)$$

the summation here is over the constituents of  $D_2^+$  ( $\alpha = 1, 2$  referring to nuclei 1 and 2, and  $\alpha = 3$  labeling the electron),  $Z_{\alpha} e$  is the corresponding electric charge.  $\hat{T}^{(2)}$  is a tensor of rank 2 with Cartesian components

$$\hat{T}_{ij}^{(2)} = \frac{1}{2} (\hat{k}_i \hat{\epsilon}_j + \hat{k}_j \hat{\epsilon}_i), \quad \hat{\mathbf{k}} \cdot \hat{\epsilon} = 0, \quad (17)$$

where  $\hat{\mathbf{k}} = \mathbf{k}/|\mathbf{k}|$ , and  $\hat{\epsilon}$  is a unit vector of polarization,  $\mathbf{E}_0 = \hat{\epsilon} |\mathbf{E}_0|$ . The Einstein's convention for summation over repeated pairs of indices of cartesian components of vectors and tensors is assumed in Eq. (15) and further on.

To switch from Cartesian to cyclic coordinates and back for the symmetric tensor operators of rank 2, we use a convention:  $Q_0^{(2)} = Q_{zz}^{(2)}$ , that implies

$$T_{ij}^{(2)} Q_{ij}^{(2)} = \frac{3}{2} \sum_q (-1)^q T_q^{(2)} Q_{-q}^{(2)} = \frac{3}{2} (T^{(2)} \cdot Q^{(2)}).$$

Note that, in a general case of elliptic polarization, the vector  $\hat{\epsilon}$ , and tensor  $\hat{T}^{(2)}$  are complex. The matrix elements of the scalar product  $\hat{T}^{(2)} \cdot Q^{(2)}$  in Eq. (15) have the form

$$\begin{aligned} \langle \Psi^{(v'L')I'F'J'_z} | \hat{T}_{ij}^{(2)} Q_{ij}^{(2)} | \Psi^{(vL)IFJJ_z} \rangle &= \frac{3}{2} \sqrt{2J+1} \times \\ &\sum_q \hat{T}^{(2)q} C_{JJ_z, 2q}^{J'J'_z} \left[ \sum_{I_1 F_1} (-1)^{J+L+F_1} \left\{ \begin{matrix} L & F_1 & J \\ J' & 2 & L' \end{matrix} \right\} \beta_{I_1 F_1}^{(vL)IFJ} \beta_{I_1 F_1}^{(v'L')I'F'J'} \right] \langle v'L' || Q^{(2)} || vL \rangle, \quad q = J'_z - J_z, \end{aligned} \quad (18)$$

and similar for the conjugate one, where  $\langle v'L' || Q^{(2)} || vL \rangle$  are the reduced matrix elements of  $Q^{(2)}$ . The Rabi frequency for the transition  $|i\rangle \rightarrow |f\rangle$  is expressed in terms of these matrix elements as follows

$$\Omega_{if} = \frac{\omega_{if} |\mathbf{E}_0|}{3\hbar c} \langle \Psi^{(v'L')I'F'J'_z} | \hat{T}_{ij}^{(2)} Q_{ij}^{(2)} | \Psi^{(vL)IFJJ_z} \rangle \quad (19)$$

where  $\omega_{if} = (E^{(v'L')I'F'J'} - E^{(vL)IFJ})/\hbar$ . Note that for general polarization  $\Omega_{if}$  is complex. The probability per unit time  $\mathcal{W}_{if}$  for the transition  $|i\rangle \rightarrow |f\rangle$ , stimulated by the external electric field with amplitude  $\mathbf{E}_0$ , oscillating with frequency  $\omega$  and propagating along  $\mathbf{k}$ , may be expressed in terms of the Rabi frequency as follows:  $\mathcal{W}_{if} = 2\pi(\delta(\omega - \omega_{if}) + \delta(\omega + \omega_{if})) |\Omega_{if}|^2$ . We shall put it in the factorized form used in Eq. (18) of [10]:

$$\mathcal{W}_{if} = \mathcal{W}^{\text{NR}}(v'L'; vL) \mathcal{W}^{\text{hfs}}((v'L')I'F'J'; (vL)IFJ) \mathcal{W}^{\text{pol}}(J'_z; J_z). \quad (20)$$

The first factor,  $\mathcal{W}^{\text{NR}}(v'L'; vL)$ , is the rate of stimulated  $E2$  transitions in  $D_2^+$  in the non-relativistic (spinless) approximation, averaged over the initial and summed over the final angular momentum projections  $L_z, L'_z$

$$\mathcal{W}^{\text{NR}}(v'L'; vL) = \frac{\pi \omega_{if}^2}{\epsilon_0 c^3 \hbar^2} \frac{1}{15(2L+1)} \left| \langle v'L' || Q^{(2)} || vL \rangle \right|^2 \bar{\mathcal{I}}, \quad \bar{\mathcal{I}} = \int d\omega \mathcal{I}(\omega) g_{if}(\omega), \quad (21)$$

where  $\mathcal{I}(\omega)$  is the spectral density of the external (laser) field energy flux, and  $g_{if}(\omega)$  is the transition line spectral profile. The factor

$$\mathcal{W}^{\text{hfs}}((v'L')I'F'J'; (vL)IFJ) = (2L+1)(2J'+1) \left( \sum_{I_1 F_1} \beta_{I_1 F_1}^{(v'L')I'F'J'} \beta_{I_1 F_1}^{(vL)IFJ} (-1)^{J+F_1} \left\{ \begin{matrix} L & F_1 & J \\ J' & 2 & L' \end{matrix} \right\} \right)^2, \quad (22)$$

describes the intensity of the individual hyperfine component  $IFJ \rightarrow I'F'J'$  of the transition line  $(vL) \rightarrow (v'L')$ . Because of the weak mixing of the pure states in Eq. (13) (see Tables III,IV) a good approximation for the intensity of the strong (favored) transitions is to assume that  $\beta_{I'F'}^{(vL)IFJ} \approx \delta_{I'I} \delta_{F'F}$  that leads to

$$\mathcal{W}^{\text{hfs}}((v'L')IFJ'; (vL)IFJ) \approx (2L+1)(2J'+1) \left\{ \begin{matrix} L & F & J \\ J' & 2 & L' \end{matrix} \right\}^2. \quad (23)$$

The weak (unfavored) transitions are forbidden in this approximation.

Finally

$$\mathcal{W}^{\text{pol}}(J'J'_z; JJ_z) = \frac{15(2J+1)}{2J'+1} \left( C_{JJ_z, 2q}^{J'J'_z} \right)^2 \left| \hat{T}_q^{(2)} \right|^2, \quad q = J'_z - J_z, \quad (24)$$

is related to the intensity of the Zeeman components of a hyperfine transition line with different values of the magnetic quantum numbers  $J_z, J'_z$ .  $\mathcal{W}^{\text{pol}}(J'J'_z; JJ_z)$  is normalized with the condition

$$\frac{1}{2J+1} \sum_{J_z; J'_z} \mathcal{W}^{\text{pol}}(J'J'_z; JJ_z) = 1. \quad (25)$$

Note that compared with Eqs. (20)-(21) of Ref. [10], the factor  $(2J+1)$  has now been moved from  $\mathcal{W}^{\text{hfs}}$  to  $\mathcal{W}^{\text{pol}}$ . In absence of external magnetic field or in case of spectral resolution insufficient to distinguish the Zeeman components, the rate  $\mathcal{W}_1$  of excitation of an individual hyperfine component  $J_z$  to any of the Zeeman states  $J'_z$  is independent of  $J_z$ , and using Eqs. Eq. (20),(25) is reduced to  $\mathcal{W}_1 = \mathcal{W}^{\text{NR}}(v'L'; vL) \mathcal{W}^{\text{hfs}}((v'L')I'F'J'; (vL)IFJ)$ . Similarly, the product  $\mathcal{W}^{\text{hfs}}((v'L')I'F'J'; (vL)IFJ) \mathcal{W}^{\text{pol}}(J'J'_z; JJ_z)$  satisfies the normalization condition

$$\sum_{I'F'J'J'_z} \frac{1}{n^{\text{hfs}}(vL)} \sum_{IFJJ_z} \mathcal{W}^{\text{hfs}}((v'L')I'F'J'; (vL)IFJ) \mathcal{W}^{\text{pol}}(J'J'_z; JJ_z) = 1, \quad (26)$$

where the sum is over the allowed values of  $I, I'$  with the same parity as  $L$ , and  $n^{\text{hfs}}(vL)$  is the number of states in the considered hyperfine manifold of the  $(vL)$  state:

$$n^{\text{hfs}}(vL) = \begin{cases} 6(2L+1) & \text{for odd } L, \\ 12(2L+1) & \text{for even } L. \end{cases} \quad (27)$$

In case the hyperfine structure of the  $E2$  transition line is not resolved, the excitation rate  $\mathcal{W}_2$  from any of the  $n^{\text{hfs}}(vL)$  initial states to all final states is found by summing  $\mathcal{W}_{if}$  of Eq. (20) over all final states and averaging over all initial states. The result is  $\mathcal{W}_2 = \mathcal{W}^{\text{NR}}(v'L'; vL)$ .

## B. Laser polarization effects on the Zeeman structure of $E2$ spectra

Recent progress in the precision spectroscopy of hydrogen molecular ions [22] has allowed to resolve the Zeeman structure of laser induced  $E1$  transition lines. Encouraged by this, we consider in details the effects of the polarization of the stimulating laser light on the Zeeman structure of  $E2$  transition lines, as described by the factor  $\mathcal{W}^{\text{pol}}(J'J'_z; JJ_z)$  in (20). These effects have an impact on the intensity and not on the frequency of the  $E2$  transitions; the calculations of the Zeeman shift of the transition frequencies will be published elsewhere.

The cyclic components of the rank-2 irreducible tensor  $\hat{T}^{(2)}$  (17) are expressed in terms of the cartesian components as follows:

$$\begin{aligned} \hat{T}^{(2)\pm 2} &= \sqrt{\frac{1}{6}} \left( \hat{k}_x \hat{\epsilon}_x - \hat{k}_y \hat{\epsilon}_y \mp i \left( \hat{k}_x \hat{\epsilon}_y + \hat{k}_y \hat{\epsilon}_x \right) \right) \\ \hat{T}^{(2)\pm 1} &= \sqrt{\frac{1}{6}} \left( \mp \left( \hat{k}_x \hat{\epsilon}_z + \hat{k}_z \hat{\epsilon}_x \right) + i \left( \hat{k}_z \hat{\epsilon}_y + \hat{k}_y \hat{\epsilon}_z \right) \right) \\ \hat{T}^{(2)0} &= \frac{1}{3} \left( 2\hat{k}_z \hat{\epsilon}_z - \hat{k}_x \hat{\epsilon}_x - \hat{k}_y \hat{\epsilon}_y \right) = \hat{k}_z \hat{\epsilon}_z. \end{aligned} \quad (28)$$

We have updated the normalization of these components as compared with Ref. [10], but have kept unchanged the parametrization of the complex unit vector  $\hat{\epsilon} = \mathbf{E}_0/|\mathbf{E}_0|$  pointing along the electric field amplitude  $\mathbf{E}_0$ . As in [10], we denote by  $K$  the lab reference frame with  $z$ -axis along the external magnetic field  $\mathbf{B}$ , by  $K'$  a reference frame with  $z$ -axis along  $\hat{\mathbf{k}}$ , and take the cartesian coordinates  $(\epsilon'_x, \epsilon'_y, \epsilon'_z)$  of  $\hat{\epsilon}$  in  $K'$  to be  $(\cos \theta, \sin \theta e^{i\varphi}, 0)$ . Linear polarization of the incident light is described by  $\varphi = 0$ ; left/right circular polarization – by  $\varphi = \pm\pi/2, \theta = \pi/4$ ; all other combinations correspond to general elliptic polarization. Let  $(\alpha, \beta, \gamma)$  be the Euler angles of the rotation that transforms  $K$  into  $K'$ , and denote by  $M(\alpha, \beta, \gamma)$  the matrix relating the cartesian coordinates  $(a_x, a_y, a_z)$  and  $(a'_x, a'_y, a'_z)$  of an arbitrary vector  $\mathbf{a}$  in  $K$  and  $K'$ , respectively:  $a_i = \sum_j M_{ij}(\alpha, \beta, \gamma) a'_j$ . (To avoid mismatch of  $M$  with  $M^{-1}$ , note that, e.g.

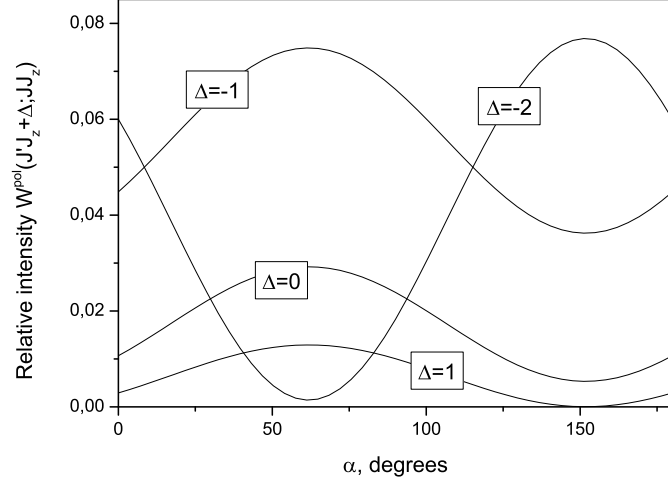


FIG. 2: Relative intensities  $W^{\text{pol}}(J'J'_z; JJ_z)$  of the Zeeman components  $(JJ_z) = (\frac{1}{2}\frac{1}{2}) \rightarrow (J'J'_z) = (\frac{3}{2}\frac{1}{2} + \Delta)$ ,  $\Delta = -2, \dots, 1$  as function of  $\alpha$  for randomly selected fixed values of the angles  $\beta = 72^\circ$ ,  $\theta = 56^\circ$ ,  $\varphi = 51^\circ$  (cf. Eq. (29))

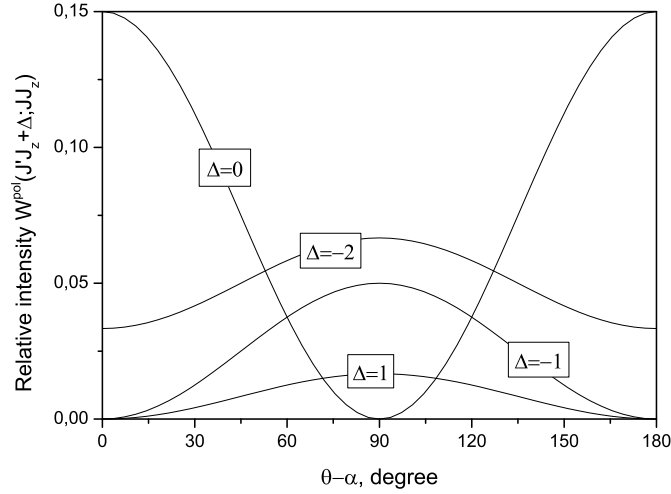


FIG. 3: Relative intensities  $W^{\text{pol}}(J'J'_z; JJ_z)$  of the Zeeman components  $(JJ_z) = (\frac{1}{2}\frac{1}{2}) \rightarrow (J'J'_z) = (\frac{3}{2}\frac{1}{2} + \Delta)$ ,  $\Delta = -2, \dots, 1$ , stimulated with linearly polarized laser light, as function of  $\theta - \alpha$  for  $\beta = 45^\circ$  (cf. Eq. (30)).

$M_{xz} = -\sin\beta \cos\gamma$ .) In this way, the absolute values of the components of  $\hat{T}$  in the lab frame  $K$ , appearing in

		$A_{v'L' \rightarrow vL} \text{ (s}^{-1}\text{)}$			
$(vL)$	$(v'L')$	$\Delta E^{\text{NR}}/hc \text{ (cm}^{-1}\text{)}$	$ \langle v'L'    Q^{(2)}    vL \rangle /ea_0^2$	This work	Pilon [8]
(00)	(02)	88.053	1.608226	0.30665[-12]	0.30665[-12]
(00)	(12)	1661.833	0.267274	0.20281[-07]	0.20281[-07]
(00)	(22)	3171.009	0.019403	0.27036[-08]	0.27036[-08]
(00)	(32)	4617.211	0.002497	0.29299[-09]	0.29298[-09]
(00)	(42)	6001.881	0.000451	0.35543[-10]	
(00)	(62)	8591.673	0.000027	0.77727[-12]	
(01)	(11)	1575.973	0.311496	0.35215[-07]	0.35215[-07]
(01)	(21)	3087.284	0.019765	0.40905[-08]	0.40905[-08]
(01)	(31)	4535.575	0.002284	0.37384[-09]	0.37382[-09]
(01)	(41)	5922.282	0.000367	0.36679[-10]	
(02)	(12)	1573.782	0.340448	0.25064[-07]	0.25064[-07]
(02)	(22)	3082.958	0.021629	0.29183[-08]	0.29182[-08]
(02)	(42)	5913.830	0.000403	0.26277[-10]	
(03)	(11)	1429.607	0.420823	0.39479[-07]	0.39479[-07]
(04)	(12)	1369.684	0.522608	0.29490[-07]	
(04)	(24)	3067.885	0.027948	0.26415[-08]	
(04)	(32)	4325.062	0.001717	0.99945[-10]	0.99939[-10]
(06)	(56)	7145.142	0.000129	0.26793[-11]	
(11)	(13)	140.894	2.379256	0.50287[-11]	0.50287[-11]
(11)	(33)	3089.955	0.048979	0.10811[-07]	0.10811[-07]
(20)	(42)	2912.431	0.052069	0.12725[-07]	
(32)	(64)	4135.286	0.024586	0.90959[-08]	
(52)	(54)	167.679	4.033412	0.26834[-10]	

TABLE V: Nonrelativistic energies,  $\Delta E^{\text{NR}} = E^{(\text{NR})v'L'} - E^{(\text{NR})vL}$ , reduced matrix elements,  $|\langle v'L' || Q^{(2)} || vL \rangle|$ , of the electrical quadrupole moments,  $Q^{(2)}$ , Eq. (16), Einstein coefficients,  $A_{v'L' \rightarrow vL}$  for selected  $E2$  transitions between the ro-vibrational states  $|vL\rangle$  and  $|v'L'\rangle$  of  $D_2^+$ , and, for comparison, the results of H.O. Pilon [8] when available.

Eq. (24) are parametrized with the *four* angles  $\alpha, \beta, \theta$ , and  $\varphi$  (the dependence on  $\gamma$  being cancelled):

$$\begin{aligned}
|\widehat{T}^{(2)\pm 2}|^2 &= -\frac{1}{12} \sin^4 \beta (1 + \cos 2\alpha \cos 2\theta + \sin 2\alpha \sin 2\theta \cos \varphi) + \\
&\quad \frac{1}{6} \sin^2 \beta (1 \pm \cos \beta \sin 2\theta \sin \varphi) \\
|\widehat{T}^{(2)\pm 1}|^2 &= \frac{1}{12} + \frac{1}{24} \cos 2\beta (1 - \cos 2\alpha \cos 2\theta) + \frac{1}{24} \cos 4\beta (1 + \cos 2\alpha \cos 2\theta) - \\
&\quad \frac{1}{12} (1 + 2 \cos 2\beta) \sin^2 \beta \sin 2\alpha \sin 2\theta \cos \varphi \pm \frac{1}{6} \cos \beta \cos 2\beta \sin 2\theta \sin \varphi \\
|\widehat{T}^{(2)0}|^2 &= \frac{1}{8} \sin^2 2\beta (1 + \cos 2\alpha \cos 2\theta + \sin 2\alpha \sin 2\theta \cos \varphi)
\end{aligned} \tag{29}$$

This leads, for linear polarization ( $\varphi = 0$ ), to

$$\begin{aligned}
|\widehat{T}_{\text{lin}}^{(2)\pm 2}|^2 &= \frac{1}{6} \sin^2 \beta (1 - \sin^2 \beta \cos^2(\theta - \alpha)) \\
|\widehat{T}_{\text{lin}}^{(2)\pm 1}|^2 &= \frac{1}{12} (1 + \cos 4\beta \cos^2(\theta - \alpha) + \cos 2\beta \sin^2(\theta - \alpha)) \\
|\widehat{T}_{\text{lin}}^{(2)0}|^2 &= \frac{1}{4} \sin^2 2\beta \cos^2(\theta - \alpha),
\end{aligned} \tag{30}$$

and for left circular polarization ( $\theta = \pi/4, \varphi = \pi/2$ )

$$\begin{aligned}
|\widehat{T}_{\text{left}}^{(2)\pm 2}|^2 &= \frac{1}{3} \sin^2 \beta \left( \frac{\cos^4 \frac{\beta}{2}}{\sin^4 \frac{\beta}{2}} \right) \\
|\widehat{T}_{\text{left}}^{(2)\pm 1}|^2 &= \frac{1}{3} (1 \mp 2 \cos \beta)^2 \left( \frac{\cos^4 \frac{\beta}{2}}{\sin^4 \frac{\beta}{2}} \right) \\
|\widehat{T}_{\text{left}}^{(2)0}|^2 &= \frac{1}{8} \sin^2 2\beta.
\end{aligned} \tag{31}$$

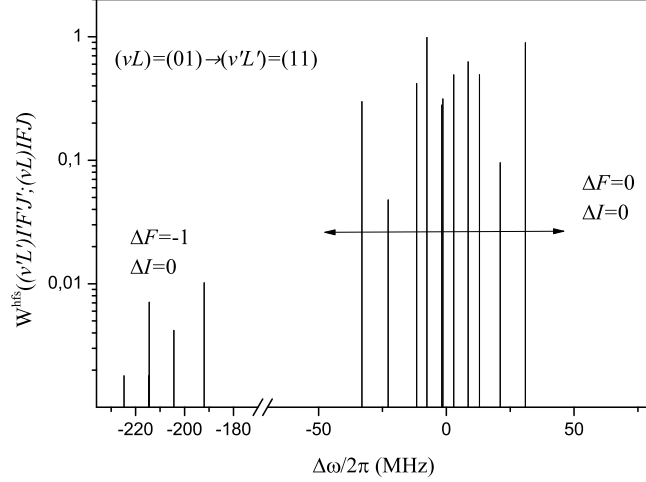


FIG. 4: Hyperfine structure of the  $|01\rangle \rightarrow |11\rangle$   $E2$  vibrational transition line. The intensity of the hyperfine components  $\mathcal{W}^{\text{hfs}}$  is plotted against the laser frequency detuning  $\Delta\omega/2\pi$  from spin-averaged transition frequency. The spectrum is dominated by the “strong” (favored) components with  $\Delta F = \Delta I = 0$ , while the intensity of transitions between hyperfine states with different  $F$  or  $I$  is suppressed by two orders of magnitude. The spectrum also includes a number of “weak” (unfavored) transitions with  $\Delta F = +1$ , not shown on the plot.

For right circular polarization, described by  $\theta = \pi/4$ ,  $\varphi = -\pi/2$ , the values of  $|\widehat{T}_{\text{right}}^{(2)q}|^2$  are obtained from the above expressions with the substitution  $|\widehat{T}_{\text{right}}^{(2)q}|^2 = |\widehat{T}_{\text{left}}^{(2)-q}|^2$ .

One might expect the intensity of the Zeeman components of the  $E2$ -transition spectrum to depend — as in  $E1$  transitions — on three parameters only: one related to the laser polarization, and two more describing the mutual orientation of the external magnetic field  $\mathbf{B}$  and the unit vectors  $\hat{\mathbf{k}}$  and  $\hat{\mathbf{e}}$ . In fact, Eqs. (30) and (31) show that this is the case for circular and linear polarization only (when the difference  $\theta - \alpha$  appears as a single parameter) while in the general case  $\mathcal{W}^{\text{pol}}(J'J'_z; JJ_z)$  depends substantially on both angles  $\alpha$  and  $\theta$ . As an illustration, on Fig. 2 are plotted the relative intensities of the Zeeman components  $|(vL)IFJ, J_z\rangle = |(00)0\frac{1}{2}\frac{1}{2}\rangle \rightarrow |(12)0\frac{1}{2}\frac{3}{2}, \frac{1}{2} + \Delta\rangle$ ,  $\Delta = -2, -1, 0, 1$  as functions of  $\alpha$  for the randomly selected values  $\beta = 72^\circ$ ,  $\theta = 56^\circ$ ,  $\varphi = 51^\circ$ . The plot shows that the measurement of one or other individual Zeeman component of  $E2$  transition lines may be substantially enhanced with appropriate optimization of the set-up geometry using Eqs. (29)-(31). The rather sharp dependence of the intensity of the individual Zeeman components on  $\theta - \alpha$  for linear polarization and fixed value of the angle  $\beta$  between  $\mathbf{B}$  and the laser propagation direction (cf. Eq. (30)) is shown in Fig. 3.

### C. Numerical results

The rate  $\mathcal{W}^{\text{NR}}(v'L'; vL)$  of laser stimulated  $E2$  transitions between the ro-vibrational states  $|vL\rangle$  and  $|v'L'\rangle$  of the molecular ion  $\text{D}_2^+$  are expressed in Eq. (21) in terms of the reduced matrix elements  $\langle v'L' || Q^{(2)} || vL \rangle$  of the electric quadrupole moment of  $\text{D}_2^+$  between these states. In the present work the reduced matrix elements were evaluated using the non-relativistic wave functions of  $\text{D}_2^+$  calculated in the variational approach of Ref. [16]. The numerical values needed for the evaluation of the rate of  $E2$  transitions between a few selected ro-vibrational states are given in Table V. For these transitions the table also lists the values of the Einstein’s coefficients  $A_{v'L' \rightarrow vL}$ , which are related to the reduced matrix elements by

$$A_{v'L' \rightarrow vL}/t_0^{-1} = \frac{\alpha^5}{15(2L+1)} ((E^{\text{NR}v'L'} - E^{\text{NR}vL})/\mathcal{E}_0)^5 (\langle v'L' || Q^{(2)} || vL \rangle / ea_0^2)^2, \quad (32)$$

where  $a_0$ ,  $t_0 = a_0/\alpha c$ , and  $\mathcal{E}_0 = 2\text{Ry}$  are the atomic units of length, time, and energy. The comparison with the values calculated by H. O. Pilon [8] with different methods for a partly overlapping selection of transitions shows good agreement for the lower excited states, and indications of possible discrepancy of the order of  $10^{-4}$  for the higher

$I$	$F$	$J$	$J'$	$\Delta E^{\text{hfs}}$ (MHz)	$\mathcal{W}^{\text{hfs}}$	$(d\Delta E^{\text{hfs}}/dQ_d)/h$ (kHz fm $^{-2}$ )
$(vL) = (00) \rightarrow (v'L') = (02)$						
2	5/2	5/2	1/2	-40.018	0.06648	-81.29
0	1/2	1/2	3/2	-32.093	0.40000	0.01
2	5/2	5/2	3/2	-25.426	0.13244	-33.21
2	3/2	3/2	7/2	-12.456	0.39882	-22.25
2	5/2	5/2	5/2	-6.961	0.19868	26.03
2	3/2	3/2	5/2	-2.633	0.29802	51.38
2	5/2	5/2	7/2	9.461	0.26588	50.39
2	3/2	3/2	3/2	11.084	0.19866	5.06
<b>2</b>	<b>5/2</b>	<b>5/2</b>	<b>9/2</b>	<b>17.331</b>	<b>0.33333</b>	<b>-28.14</b>
<b>0</b>	<b>1/2</b>	<b>1/2</b>	<b>5/2</b>	<b>21.395</b>	<b>0.60000</b>	<b>-0.02</b>
2	3/2	3/2	1/2	22.814	0.09973	-66.45
$(vL) = (00) \rightarrow (v'L') = (12)$						
2	5/2	5/2	1/2	-40.975	0.06649	-81.19
0	1/2	1/2	3/2	-30.692	0.40000	0.01
2	5/2	5/2	3/2	-27.065	0.13249	-33.07
2	5/2	5/2	5/2	-9.415	0.19875	26.07
2	3/2	3/2	7/2	-7.846	0.39886	-22.19
2	3/2	3/2	5/2	1.587	0.29812	51.32
2	5/2	5/2	7/2	6.318	0.26591	50.33
<b>2</b>	<b>5/2</b>	<b>5/2</b>	<b>9/2</b>	<b>13.883</b>	<b>0.33333</b>	<b>-28.13</b>
2	3/2	3/2	3/2	14.702	0.19873	4.92
<b>0</b>	<b>1/2</b>	<b>1/2</b>	<b>5/2</b>	<b>20.461</b>	<b>0.60000</b>	<b>-0.02</b>
2	3/2	3/2	1/2	25.879	0.09974	-66.51
$(vL) = (00) \rightarrow (v'L') = (22)$						
2	5/2	5/2	1/2	-41.846	0.06651	-80.80
0	1/2	1/2	3/2	-29.338	0.40000	0.01
2	5/2	5/2	3/2	-28.592	0.13254	-32.80
2	5/2	5/2	5/2	-11.730	0.19881	26.02
2	3/2	3/2	7/2	-3.474	0.39892	-22.05
2	5/2	5/2	7/2	3.337	0.26595	50.07
2	3/2	3/2	5/2	5.582	0.29821	51.07
<b>2</b>	<b>5/2</b>	<b>5/2</b>	<b>9/2</b>	<b>10.606</b>	<b>0.33333</b>	<b>-28.02</b>
2	3/2	3/2	3/2	18.115	0.19881	4.76
<b>0</b>	<b>1/2</b>	<b>1/2</b>	<b>5/2</b>	<b>19.559</b>	<b>0.60000</b>	<b>-0.02</b>
2	3/2	3/2	1/2	28.759	0.09976	-66.32
$(vL) = (01) \rightarrow (v'L') = (11)$						
1	3/2	5/2	1/2	-33.061	0.29815	50.33
1	3/2	3/2	1/2	-22.787	0.04784	102.72
1	3/2	5/2	3/2	-11.612	0.41821	-52.32
1	1/2	1/2	3/2	-7.593	0.98593	13.69
<b>1</b>	<b>3/2</b>	<b>5/2</b>	<b>5/2</b>	<b>-1.754</b>	<b>0.28000</b>	<b>-0.00</b>
1	3/2	3/2	3/2	-1.339	0.31375	0.07
1	1/2	1/2	1/2	-0.353	0.00000	-0.33
1	3/2	1/2	1/2	2.467	0.00000	0.31
1	1/2	3/2	3/2	2.914	0.49218	-0.06
1	3/2	3/2	5/2	8.519	0.62718	52.39
1	1/2	3/2	1/2	12.973	0.49305	-13.44
1	3/2	1/2	3/2	21.096	0.09564	-102.97
1	3/2	1/2	5/2	30.954	0.89412	-50.66

TABLE VI: The hyperfine shifts  $\Delta E^{\text{hfs}}/h = (\Delta E^{\text{hfs}(v'L')IFJ'} - \Delta E^{\text{hfs}(vL)IFJ})/h$ , in MHz, the relative intensities  $\mathcal{W}^{\text{hfs}} = \mathcal{W}^{\text{hfs}}((v'L')IFJ'; (vL)IFJ)$ , and the derivative  $(d\Delta E^{\text{hfs}}/dQ_d)/h$  in (kHz fm $^{-2}$ ) for the "strong" (favored) components in the hyperfine spectrum of two  $E2$  transitions in  $D_2^+$ . The transitions between stretched states are shown in boldface.

vibrational excitations. Juxtaposition with the analogous Table II of Ref. [10] shows that the rates of spontaneous transitions in  $D_2^+$  are suppressed in comparison with  $H_2^+$ . This is mainly due to the smaller rotational and vibrational excitation energies, related to the larger nuclear mass. In addition to Table V the electronic supplement to the present paper gives the list of the reduced matrix elements for all  $E2$  transitions between the ro-vibrational states with  $v \leq 10$  and  $L \leq 4$ .

Further on, using the values of the amplitudes  $\beta_{I'F'}^{(vL)IFJ}$ , obtained by diagonalization of the effective spin Hamiltonian matrix (14), we calculated the coefficients  $\mathcal{W}^{\text{hfs}}((v'L')I'F'J'; (vL)IFJ)$ , in the expression (20) for the rate of the individual hyperfine components. Fig. 4 illustrates the hyperfine structure of the  $E2$  transition  $|01\rangle \rightarrow |11\rangle$  and is representative also for other ro-vibrational transitions.

The spectrum consists of “strong” (favored) components between hyperfine states with the same values of the quantum numbers  $F$  and  $I$  spread over a range up to  $\pm 50$  MHz around the center of gravity of the hyperfine manifold, and “weak” components between states with  $\Delta F \neq 0$  or  $\Delta I \neq 0$  at a distance of a few hundred MHz. The weak components are suppressed due to the relatively weak mixing of  $F$  and  $I$  in the eigenstate of the effective spin Hamiltonian matrix. Compared to  $H_2^+$ , however, the suppression in  $D_2^+$  is less pronounced; the reason is that, because of the smaller nuclear magnetic moment of the deuteron, the contact spin-spin interactions dominate to a lesser extent thus leaving room for more  $F$  and  $I$  mixing.

Table VI lists the details of the “strong” (favored) hyperfine components of four selected  $E2$  transition lines: one rotational transition, two fundamental vibrational transitions, and one vibrational overtone transition. The electronic supplement includes a table of the hyperfine structure of all  $E2$  transition lines between the ro-vibrational states with  $v \leq 10$  and  $L \leq 4$ .

#### IV. CONCLUSION

The present paper reports a series of new theoretical results about the spectroscopy of the molecular ion  $D_2^+$ , including the most accurate to date calculations of the hyperfine structure of the lower excited ro-vibrational states with vibrational and rotational quantum numbers  $v \leq 10$ ,  $L \leq 4$ . The correct theoretical treatment of the hyperfine structure is essential, considering that the experimental uncertainty of the measurement of the hyperfine structure has already reached the 20 Hz level in one of the molecular hydrogen ions [22]. The paper also presents the first evaluation of the hyperfine structure of the  $E2$  ro-vibrational transitions, and a thorough consideration of the laser polarization effects in the laser spectroscopy of the resolved Zeeman components of the hyperfine transition lines. The work closely followed, but also further developed the formalism of Ref. [10] for the study of the electric quadrupole transition spectrum of  $H_2^+$ . It is hoped that the present results open the perspective for performing precision spectroscopy also on  $D_2^+$  in the near future. Apart from the well-known goals of mass ratio determination and test of QED, the spectroscopy of  $D_2^+$  specifically opens the possibility of searching for an anomalous force between deuterons [24], and the precision measurement of the electric quadrupole moment of the deuteron.

#### Acknowledgments

D.B. and P.D. gratefully acknowledge the support of Bulgarian National Science Fund under Grant No. FNI 08-17. V.I.K. acknowledges support from the Russian Foundation for Basic Research under Grant No. 19-02-00058-a. S.S. acknowledges support from the European Research Council (ERC) under the European Union Horizon 2020 research and innovation programme (grant agreement No. 786306).

- 
- [1] S. Alighanbari, M.G. Hansen, S. Schiller, and V.I. Korobov, *Rotational spectroscopy of cold and trapped molecular ions in the Lamb-Dicke regime*, Nature Physics **14**, 555 (2018).
  - [2] Sayan Patra, J.-Ph. Karr, L. Hilico, M. Germann, V.I. Korobov, and J.C.J. Koelemeij, *Proton-electron mass ratio from  $HD^+$  revisited*, J. Phys. B: At. Mol. Opt. Phys. **51**, 024003 (2018).
  - [3] S. Schiller, D. Bakalov, and V.I. Korobov, *Simplest Molecules as Candidates for Precise Optical Clocks*, Phys. Rev. Lett. **113**, 023004 (2014).
  - [4] J.-Ph. Karr, L. Hilico, J. C. J. Koelemeij, and V. I. Korobov, *Hydrogen molecular ions for improved determination of fundamental constants*, Phys. Rev. A **94**, 050501 (2016).
  - [5] D.R. Bates and G. Poots, *Properties of the Hydrogen Molecular Ion I: Quadrupole Transitions in the Ground Electronic State and Dipole Transitions of the Isotopic Ions*, Proc. Phys. Soc. A **66**, 784 (1953).

- [6] A. G. Posen, A. Dalgarno, and J. M. Peek, *The quadrupole vibration-rotation transition probabilities of the molecular hydrogen ion*, At. Data Nucl. Data Tables **28**, 265 (1983).
- [7] H.O. Pilón and D. Baye, *Quadrupole transitions in the bound rotational-vibrational spectrum of the hydrogen molecular ion*, J. Phys. B: At. Mol. Opt. Phys. **45**, 065101 (2012).
- [8] H.O. Pilón, *Quadrupole transitions in the bound rotational-vibrational spectrum of the deuterium molecular ion*, J. Phys. B: At. Mol. Opt. Phys. **46**, 245101 (2013).
- [9] J.-Ph. Karr,  *$H_2^+$  and  $HD^+$ : Candidates for a molecular clock*, J. Mol. Spectrosc. **300**, 37 (2014).
- [10] V.I. Korobov, P. Danev, D. Bakalov, and S. Schiller, *Laser-stimulated electric quadrupole transitions in the molecular hydrogen ion  $H_2^+$* , Phys. Rev. A **97**, 032505 (2018).
- [11] P. Zhang, Z. Zhong, and Z. Yan, *Contribution of the deuteron quadrupole moment to the hyperfine structure of  $D_2^+$* , Phys. Rev. A **88**, 032519 (2013).
- [12] P. Zhang, Z. Zhong, Z. Yan, and T. Shi, *Precision spectroscopy of the hydrogen molecular ion  $D_2^+$* , Phys. Rev. A **93**, 032507 (2016).
- [13] J.F. Babb and A. Dalgarno, *Spin coupling constants and hyperfine transition frequencies for the hydrogen molecular ion*, Phys. Rev. A **46**, 9 (1992).
- [14] D. Bakalov, S. Schiller, and V.I. Korobov, *High-Precision Calculation of the Hyperfine Structure of the  $HD^+$  Ion*, Phys. Rev. Lett. **97**, 243001 (2006).
- [15] D. Bakalov, V.I. Korobov, and S. Schiller, *Magnetic field effects in the transitions of the  $HD^+$  molecular ion and precision spectroscopy*. J. Phys. B: At. Mol. Opt. Phys. **44**, 025003 (2011).
- [16] V.I. Korobov, D. Bakalov, and H.J. Monkhorst, *Variational expansion for antiprotonic helium atoms*, Phys. Rev. A **59**, R919(R) (1999).
- [17] <https://physics.nist.gov/cuu/Constants/index.html>.
- [18] M. Pavanello, W. C. Tung, and L. Adamowicz, *Determination of deuteron quadrupole moment from calculations of the electric field gradient in  $D_2$  and  $HD$* , Phys. Rev. A **81**, 042526 (2010).
- [19] H. Jozwiak\*, H. Cybulski, P. Wcislo, *Hyperfine components of all rovibrational quadrupole transitions in the  $H_2$  and  $D_2$  molecules*, arXiv:2006.05717 (2020).
- [20] J. Komasa, M. Puchalski, and K. Pachucki, *Hyperfine structure in the  $HD$  molecule*, arXiv:2005.02702 (2020).
- [21] N.J. Stone, *Table of nuclear magnetic dipole and electric quadrupole moments*, Atomic Data and Nuclear Data Tables **90**, 75 (2005).
- [22] S. Alighanbari, G.S. Giri, F.L. Constantin, V.I. Korobov, and S. Schiller, *Precise test of quantum electrodynamics and determination of fundamental constants with  $HD^+$  ions*, Nature **580**, 152 (2020), doi: <https://doi.org/10.1038/s41586-020-2261-5>.
- [23] J. F. Babb, Current Topics in Physics, eds. Y.M. Cho, J. B. Hong, and C. N. Yang (World Scientific, Singapore, 1998), p. 531.
- [24] E.J. Salumbides, W. Ubachs, and V.I. Korobov, *Bounds on fifth forces at the sub- $\text{\AA}$  length scale*, J. Mol. Spectrosc. **300**, 65 (2014).



The supplemental material includes the following five ASCII files with tables that were only partly presented in the text of the paper:

1. `d2plus-Heff.lst` with the coefficients  $E_n, n = 1, \dots, 6$  of the effective spin Hamiltonian  $H^{\text{eff}}$  of  $D_2^+$  in the ro-vibrational states with orbital momentum  $L = 1, \dots, 4$  and vibrational quantum number  $v \leq 10$ .
2. `d2plus-hfs-evnL.lst` with the hyperfine shift  $\Delta E^{(vL)IFJ}$ , the mixing coefficients  $\beta_{I'F'}^{(vL)IFJ}$ , and the derivative of the hyperfine shift with respect to the deuteron electric quadrupole moment,  $d\Delta E^{(vL)IFJ}/dQ_d$ , for states with  $v \leq 10$  and *even* values of the orbital momentum  $L = 0, 2, 4$ .
3. `d2plus-hfs-oddL.lst` with the hyperfine shift  $\Delta E^{(vL)IFJ}$ , the mixing coefficients  $\beta_{I'F'}^{(vL)IFJ}$ , and the derivative of the hyperfine shift with respect to the deuteron electric quadrupole moment,  $d\Delta E^{(vL)IFJ}/dQ_d$ , for states with  $v \leq 10$  and *odd* values of the orbital momentum  $L = 1, 3$ .
4. `d2plus-E2-evnL.lst` with the hyperfine shift  $\Delta E^{\text{hfs}}$ , its derivative with respect to  $Q_d$ ,  $d\Delta E^{\text{hfs}}/dQ_d$ , and the relative intensity  $\mathcal{W}^{\text{hfs}} = \mathcal{W}^{\text{hfs}}((v'L')IFJ'; (vL)iFJ)$  of the strong (favored) hyperfine components of the  $E2$ -transition lines between states with  $v \leq 10$  and *even* values  $L \leq 4$ .
5. `d2plus-E2-oddL.lst` with the hyperfine shift  $\Delta E^{\text{hfs}}$ , its derivative with respect to  $Q_d$ ,  $d\Delta E^{\text{hfs}}/dQ_d$ , and the relative intensity  $\mathcal{W}^{\text{hfs}} = \mathcal{W}^{\text{hfs}}((v'L')IFJ'; (vL)iFJ)$  of the strong (favored) hyperfine components of the  $E2$ -transition lines between states with  $v \leq 10$  and *odd* values  $L \leq 4$ .

The above ASCII files contain uniformly formatted lines without any special symbols. The data in each line are separated by one or more spaces and appear in the order described below.

1. `d2plus-Heff.lst`

The file contains 55 lines. In each line are given the quantum numbers  $v$  and  $L$  (integers), and the six coefficients  $E_n, n = 1, \dots, 6$  in units of MHz.

2. `d2plus-hfs-evnL.lst`

Each of the 286 lines contains the description of one hyperfine component, as follows:

- the ordinal number of the line;
- the quantum numbers  $v$  and  $L$  (integers);
- the quantum numbers of the hyperfine component  $I, F$ , and  $J$  (printed as real numbers);
- the hyperfine shift  $\Delta E^{(vL)IFJ}/h$ , in MHz;
- the five expansion coefficients  $\beta_{I'F'}^{(vL)IFJ}$ ;
- the derivative  $d\Delta E^{(vL)IFJ}/dQ_d$ , in kHz fm<sup>-2</sup>.

3. `d2plus-Heff.lst`

Same as `d2plus-hfs-evnL.lst`, with a total of 121 lines.

4. `d2plus-E2-evnL.lst`

For each allowed  $E2$  transition  $(vL) \rightarrow (v'L')$  between rovibrational states with  $v, v' \leq 10$  and *even* values of the orbital momentum  $L, L' \leq 4$ , are given:

- a title line with the non-relativistic quantum numbers of the initial and final states in the form " $(v, L) \rightarrow (v'L')$ ";
- the characteristics of the strong (favored) hyperfine components  $|(vL)IFJ\rangle \rightarrow |(v'L')IFJ'\rangle$  in increasing order of the hyperfine shift  $\Delta E^{\text{hfs}} = \Delta E^{(v'L')IFJ'} - \Delta E^{(vL)IFJ}$ , including:
  - the quantum numbers  $I$  (integer), and  $F, J, J'$  (real);
  - the hyperfine shift  $\Delta E^{\text{hfs}}/h$  in MHz;
  - the relative intensity  $\mathcal{W}^{\text{hfs}}((v'L')IFJ'; (vL)iFJ)$ ;
  - the derivative  $d\Delta E^{\text{hfs}}/dQ_d$ , in kHz fm<sup>-2</sup>.

5. `d2plus-E2-oddL.lst`

Same as `d2plus-E2-evnL.lst`, but for the allowed  $E2$  transitions between rovibrational states with  $v, v' \leq 10$  and *odd* values  $L, L' = 1, 3$ .